Cluster-Expansion Model for Complex Quinary Alloys: Application to Alnico Permanent Magnets

Manh Cuong Nguyen, Lin Zhou, Wei Tang, Matthew J. Kramer, Iver E. Anderson, Cai-Zhuang Wang, and Kai-Ming Ho

Phys. Rev. Applied **8**, 054016 — Published 8 November 2017

DOI: 10.1103/PhysRevApplied.8.054016

Cluster Expansion Model for Complex Quinary Alloy: Application to alnico Permanent Magnets

Manh Cuong Nguyen[1]*, Lin Zhou[1], Wei Tang[1], Matthew J. Kramer[1,2], Iver E. Anderson[1,2], Cai-Zhuang Wang[1,3] and Kai-Ming Ho[1,3]

[1]*Ames Laboratory, U.S. DOE, Iowa State University, Ames, IA 50011, USA*

[2]*Department of Materials Science and Engineering, Iowa State University, Ames, IA 50011, USA*

[3]*Department of Physics and Astronomy, Iowa State University, Ames, IA 50011, USA*

Abstract

An accurate and transferable cluster expansion model for complex quinary alloys was developed. Lattice Monte Carlo simulation enabled by this cluster expansion model was used to investigate temperature dependent atomic structure of alnico alloys, which have been considered as promising high performance non-rare earth permanent magnet materials for high temperature applications. The results from Monte Carlo simulations are consistent with available experiment data and provide useful insights into phase decomposition, selection and chemical ordering in alnico. The simulations also reveal a previously un-recognized $D0_3$ alloy phase. This phase is very rich in Ni and exhibits very weak magnetization. Manipulating the size and location of this phase provides a possible route to improve the magnetic properties of alnico, especially coercivity.

PACS: 61.6.Dk, 75.50.Ww, 75.75.-c, 61.50.Ah

An accurate and efficient configurational exploration scheme for complex multicomponent alloys has been considered as a difficult, long-standing problem in design of complex alloys at finite temperature. Monte Carlo simulation [1] can be used to investigate the alloys at finite temperatures. However, an efficient and accurate method for energy calculation of large size systems is a bottleneck. First-principles density functional theory (DFT) [2] calculations can give accurate energy but the computational demand is too heavy to be feasible for practicing Monte Carlo simulation for complex alloys. Cluster expansion (CE) [3,4], which mimics the well-known spin Ising-model with spin eigenvalues at each lattice sites replaced by chemical occupations of the alloy constituents, offers a possible way to address this challenge for alloys having a defined underlying lattice. The model parameters, called cluster expansion coefficients, are determined by fitting to the energies, resulted from accurate calculations (e.g. DFT), of a set of training structures. Using the CE model, the energy of an alloy supercell containing thousands of lattice sites can be calculated within sub-seconds, making Monte Carlo simulation for complex multicomponent alloys feasible.

In principle, CE model can be applied to alloys with any number of chemical elements as long as the underlying lattice is defined. In practice, the complexity of the method increases rapidly with the number of chemical elements in multicomponent alloys [4]. Most of the work with CE so far has been for binary and ternary systems [5–8] and far less has been for more components alloy systems. There are few papers employing CE for quaternary and quinary alloys published so far [9–12].

Alnico alloys were the permanent magnet (PM) materials of choice prior to the discovery of rare-earth (RE) based alloys in the 1960s. Recently, alnico has received much attention because it is a promising candidate for further development of magnets for elevated and high temperature applications [13,14]. Alnico magnets have a very small temperature dependence for their magnetic properties [14], which is highly desirable for some applications such as traction motors used in electric vehicles where the working conditions include elevated temperature 420 ~ 480 K. Alnico 8 and 9 have coercivity H_{ci} = 1900 and 1375 Oe and remanence B_r = 7.4 and 11.2 kG, respectively, and could be further enhanced by modifying the microstructure or alloying [13–15], or via magneto-thermal treatment processes. A re-design of PM motor specifically for using alnico together with an enhancement of alnico coercivity could make non-

rare earth PM vehicle motors possible in the near future. Comprehensive knowledge about the structure changes at atomic scale with annealing temperature of alnico is essential for optimizing processing to control the microstructure of alnico and, thereby, to enhance its magnetic properties.

The general understanding of alnico is that the system consists of 2 primary alloy phases, the ferromagnetic (namely, α_1) phase, rich in Fe and Co, and the "*non-magnetic*" matrix (namely, α_2) phase with Al, Ni, Co and some Fe with minor alloying elements such as Ti. Both phases have a coherent body-centered cubic (BCC) underlying lattice (the α_2 forms the $L2_1$ order which can be considered as a supercell of 8 BCC units). The segregation of the alnico master alloy into α_1 and α_2 phases arises from spinodal decomposition occurring during the cooling/quenching from a solid solution (BCC or B2) phase at very high temperature (~1523 K). The best performing alnico alloys require annealing with a magnetic field near their Curie temperature (~1113 K for ~10 mins) followed by a series of lower temperature anneals (e.g., 883 K or 863 K for few hours) [16–18] where details vary based on composition. The subsequent morphology of the spinodal varies with composition. While alnico 5 and 5-7 shows a "*brick and mortar*" pattern, alnico 8 and 9 show a "*mosaic tile*" pattern in the microstructures in a transverse section [15,19]. The purpose of the magnetic field annealing is to bias the growth of the spinodal phases along the applied field direction. The magnetic α_1 phase will form long needles separated by matrix α_2 phase in those crystals whose {100} axis is well aligned to the magnetic field. It is the magnetic shape anisotropy of the α_1 phase that is responsible for the enhanced magnetism in these alloys. The α_2 phase is believed to be a non-magnetic or weakly magnetic phase which decouples the interactions between α_1 phase needles to enhance the shape anisotropy of the α_1 needles and, hence, the coercivity of alnico.

In this work, we develop a cluster expansion model for BCC quinary alnico alloys consisting of Al, Ni, Co, Fe and Ti based on a DFT structure database. The cluster expansion model is intensively and extensively validated for temperature dependent phase separation and chemical ordering of known ternary alloys. We use lattice Monte Carlo simulation to study the phase selection and chemical ordering in alnico 8 and 9. The decomposition into α_1 magnetic and α_2 matrix phases is more complete at lower annealing temperature. We will show that there is an additional 3rd alloy phase, which is rich in Ni. Our prediction of the 3rd alloy phase is fully

supported by experimental observation with high resolution TEM. The chemical orderings and magnetic properties of all alloy phases are also investigated. The details of computational methods and model are given in the Supplementary Material [20].

We fit the CE coefficients for BCC quinary Al-Ni-Co-Fe-Ti alloy up to the 3rd nearest-neighbor (NN) pair and triplet clusters by ATAT code [4,21] to a dataset from DFT calculations [22–26]. Figure 1 shows the formation energies of the reference structures calculated by CE model versus DFT. We can see that the CE energies are very well fitted to the DFT energies. The root mean square error of this fitting is very small, 12.9 meV/atom. The cross-validation score, which measures the error in predicting energies of a set of new structures that are not included in the reference database [4], is an important indicator of the accuracy and transferability of CE coefficients. As one can see from Fig. 1, the cross-validation score is also very small (17.2 meV/atom) in our CE model. We also show in Fig. 1 the values of effective cluster interactions (ECIs) of the pair and triplet clusters obtained from our CE fitting. We can see that the 1st and 2nd NN pair interactions are the most significant whereas the ECIs of the 3rd NN pair interactions and the triplet interactions are much smaller. This indicates that further increasing the number of clusters may not be needed.

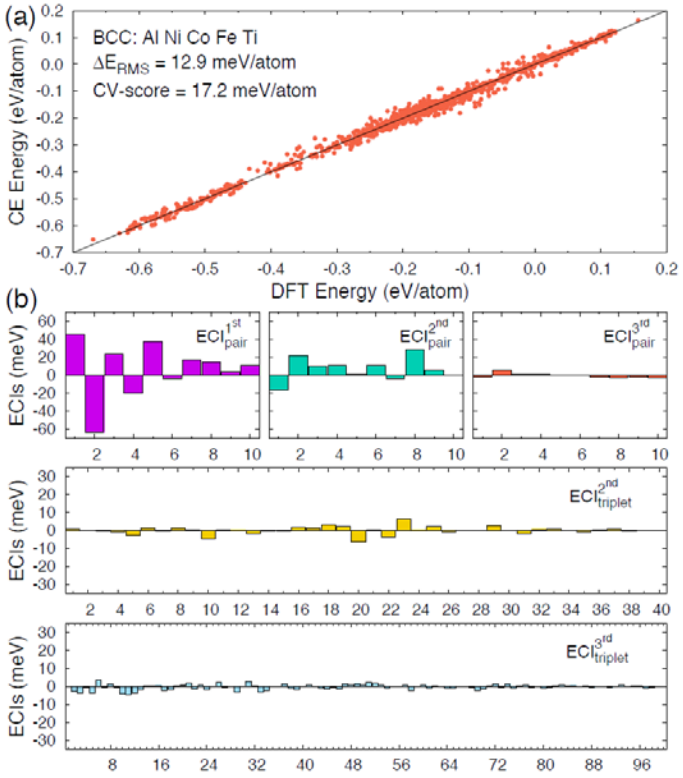

Figure 1. CE vs. DFT formation energies of database structures is shown in (a) and the values of ECIs of 1st, 2nd and 3rd NN pair and 2nd and 3rd NN triplet clusters are shown in (b). The horizontal *x*-axis stands for different clusters having different chemical decorations.

We further validate our quinary CE model in describing the phase selection and decomposition in complex alloys by performing MC simulations, for a wide range of temperature, for known BCC-based ternary alloys of Al, Ni, Co, Fe and Ti: $AlNiFe_2$, $AlCo_2Ti$ and $AlNi_2Ti$ ternary alloys. $AlNiFe_2$ is in a B2 (AlFe, NiFe) single phase at high temperature and is decomposed into BCC Fe-rich and B2 NiAl-rich phases at low temperature [27]. $AlCo_2Ti$ and $AlNi_2Ti$ are in $L2_1$ phase for a wide range of temperature [28–30]. We show in Fig. 2 the calculated compositional contour histograms, calculated from 1000 converged configurations, of $AlNiFe_2$ ternary alloy at different temperatures, 773, 1173 and 1973 K, respectively. We can see clearly that the $AlNiFe_2$ alloy is in a single phase at high temperature (1973 K) and is decomposed into 2 phases, NiAl-rich and Fe-rich phases, at lower temperature (1173 and 773 K). From the neighbor correlation tables of the $AlNiFe_2$ alloy at high (1973 K) and low (773 K) temperature (Table S.1 and S2 in Supplementary Material [20]) we find that at high temperature the $AlNiFe_2$ is in a B2 order with almost all Al atoms sitting on the α-site and almost all Ni atoms sitting on the β-site. At low temperature, the AlNi-rich phase is in B2 order with the α-site occupied mostly by Al and the β-site occupied mostly by Ni. These observations of temperature dependent phase separation, phase selection and phase ordering from our MC simulations are consistent with the experimental phase diagram [27]. However, there is an overestimation of the transition temperature from two phases to single phase of $AlNiFe_2$ alloy. The transition temperature is about 1873 K in our MC simulation while it is about 1273 K from the phase diagram. This overestimation of phase transition temperature could be traced back to several factors including the truncation of CE coefficients, the systematic error in DFT calculations and the contribution of vibrational entropy to free energy. We will not discuss in detailed about this overestimation here, since previous works already discussed about this overestimation of transition temperature, quite clearly [8,10]. Monte Carlo simulations for $AlCo_2Ti$ and $AlNi_2Ti$ ternary alloys (see Supplementary Material [20]) show that both phases are in a $L2_1$ order phase for a wide range of temperature, which is also consistent with experimental results [28–30]. Therefore, apart from an offset in transition temperature, MC simulation based on CE method

can describe phase selection and decomposition of complex alloys accurately. These results also validate the accuracy and transferability of our newly developed CE model for the quinary alloy.

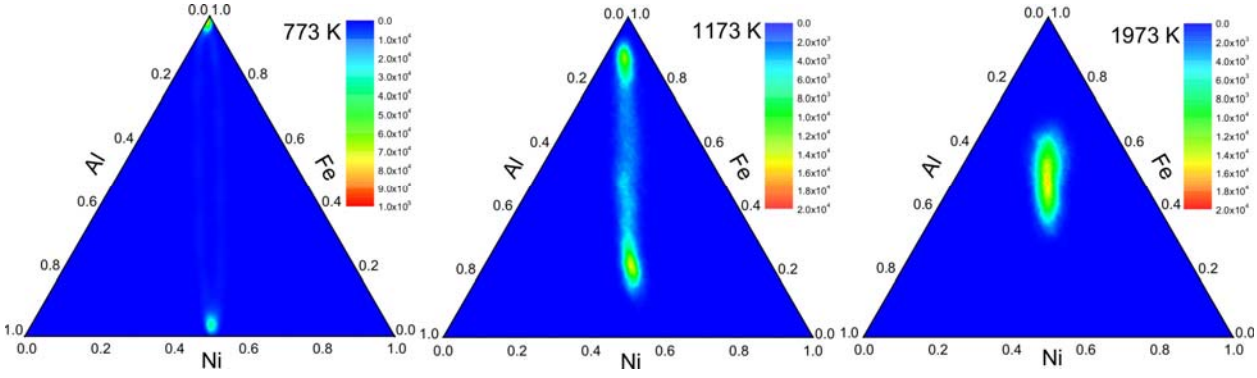

Figure 2. Compositional contour histograms showing relative composition probabilities of $AlNiFe_2$ ternary alloy at different annealing temperatures obtained from MC simulation. Histograms are calculated from 1000 converged configurations.

The chemical composition of commercial alnico 8 (without Cu), i.e., $Al_{0.140}Ni_{0.117}Co_{0.359}Fe_{0.312}Ti_{0.072}$, is used in our simulations for alnico. Figure 3 shows the compositions of phases of alnico as function of annealing temperature between 773 and 1773 K. Firstly, let's discuss the right part of the plot with temperature higher than 973 K. For temperature higher than 1573 K, the alnico master alloy is in homogenized phase with composition of each element at that of the overall composition. For temperature lower than 1573 K the alnico master alloy decomposes into 2 phases. It is interesting that the decompositions of constituent elements start at different temperatures: Al, Fe and Ti start to split their compositions first at between 1473 and 1573 K then Co and Ni start to split their compositions at between 1273 and 1373 K. The late decomposition of Co was also observed in MC simulations for alnico 5-7 [10].

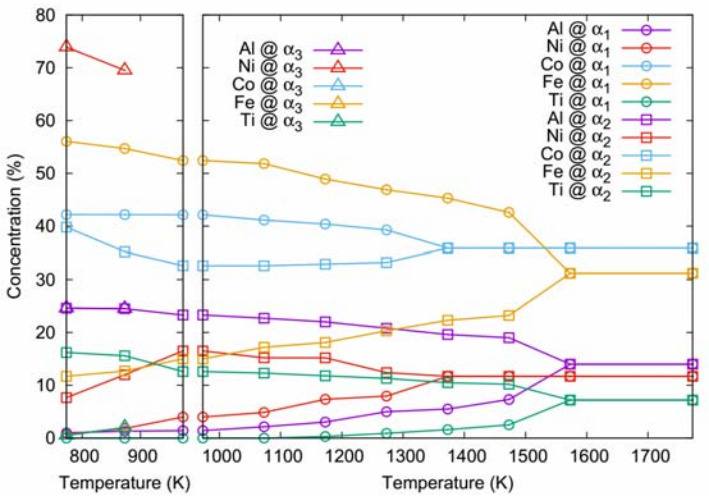

Figure 3. Composition of each element in alnico 8 as function of annealing temperature obtained from MC simulations. Circle, square and up triangle symbols are for compositions of α_1, α_2 and α_3 phases.

The two decomposed phases are the magnetic α_1 and matrix α_2 phases, respectively. From Fig. 3 we can see that the compositions of Al, Ni and Ti in α_1 phase and those of Fe and Co in α_2 phase are decreasing as the annealing temperature decreases. At lower temperature (1073 or 973 K) the compositions of Al and Ni in α_1 phase are very small and there is almost no Ti in the α_1 phase. In the α_2 phase, the compositions of Co is less but still considerable and the Fe drops off more, but goes to about half of the starting level. These results are consistent with experimental results for alnico 8 and 9: Ti is mostly residing in the α_2 phase with very small or almost no Ti in α_1 phase; the α_1 phase consists mainly of Fe and Co with small amounts of Ni and Al; concentration of Fe and Co in the α_2 phase is still significant, with Co only slightly less than in the α_1 phase. Because Ni is a very weak magnetic element, the magnetism of the magnetic α_1 phase will be enhanced if the concentration of Ni is low. On the other hand, the coercivity of alnico 8 and 9 will be enhanced if the α_2 matrix phase is less magnetic or non-magnetic to properly decouple the interactions between magnetic α_1 phase needles. Results shown in Fig. 3 imply that lowering the annealing temperature could improve the magnetic properties of alnico by enhancing magnetism of α_1 phase via increasing magnetic elements' concentrations while diminishing magnetism of α_2 phase via decreasing magnetic elements' concentrations at the same time.

The compositions of α_1 and α_2 phases obtained from MC simulations between 973 K and 1173 K are quite close to the experimental observations for alnico 8 [15], especially, the α_1 phase. There is overestimation of Fe composition and underestimation of Ni composition in the α_2 phase. The differences could be attributed to two main factors. Firstly, our MC simulation is for the equilibrium state, meaning that the observed compositions from simulation are at the boundaries of the spinodal decomposition domain. Heat treatment in an experiment is only for a short time so that the measured compositions of decomposed phases have diverged to points along the horizontal line connecting the 2 end (equilibrium) points of the spinodal decomposition domain at the given temperature, and not the end points. Secondly, although DFT is currently one of the state-of-the-art first-principles methods, it could have a systematic error in the relative stabilities of different alloy phases. For a quinary alloy, there are too many possible sub-alloy phases so that it is not feasible to trace back for the DFT systematic error and small underestimation or overestimation of compositions of constituent elements in the α1 and α2 phases are understandable and actually expected in our simulations. We also would like to note that we observed a temperature offset, in comparison with experiment, in MC simulation for ternary discussed above. A temperature offset should be also expected for alnico alloys. Since the current work is focusing on the trend of the phase decomposition and ordering in alnico 8 and 9 as function of annealing temperature rather than the exact compositions of each separated phases at a given temperature, the results obtained from our MC simulations provide very valuable information on the relative order of reactions for designing optimal heat treatment processes in experiment.

Commercial alnico 8 and 9 magnets achieve their current reproducible properties through the above mentioned complex processes that include quenching and annealing (with and without external field) at different temperatures for different periods of time [18]. This complicated process scheme came from experimental experiences accumulating over a long period of time, essentially for 70-80 years. However, the urgent need for improvement of the magnetic properties of alnico alloys for use in compact electric drive motors needs a better approach than the time-consuming blind trial-and-error experimentation efforts. A better understanding of the physics behind the current multi-step annealing processing should be the first move forward to speed up the cycle for improved magnetic properties of alnico. The results in Fig. 3 give us some key information for better understanding of the dependence of structures and magnetic properties

on the synthesis processes. As shown in Fig. 3, the spinodal decomposition can involve very significant compositional shifts, but the extent of this transformation that will take place during fast quenching and high temperature annealing depends on atomic mobility to establish the overall microstructure of "*mosaic tile*" pattern. The spinodal decomposition evolves faster at higher temperature so that the first magnetic annealing step needs to be at a high temperature (just below the spinodal onset and the Curie temperature of α_1 phase) to rapidly generate the mosaic microstructure. Unfortunately, the Co (Ni) composition is the same or very close in α_1 and α_2 phases at high temperature, meaning that Co (Ni) concentration is too high in the α_2 (α_1) phases. High Co concentration in α_2 phase can induce magnetism in α_2 phase and, hence, lower the coercivity due to poor magnetic isolation between α_1 phase needles. At the same time, high Ni concentration in the α_1 phase will lower the magnetic moment of α_1 phase. As a result, the magnetization and coercivity of alnico 8 and 9 right after high temperature magnetic annealing are low. The lower temperature annealing (draw process) has the effect of altering Ni and Co compositions in the α_1 and α_2 phases. It is desirable that these annealing steps significantly lower the un-wanted high Co concentration in the α_2 phase and the overall Ni content in the α_1 phase to enhance the magnetic properties of alnico 8 and 9. However, the spinodal decomposition evolves much slower at lower temperature so that a very long time annealing is needed to obtain the desired microstructure for good magnetic properties.

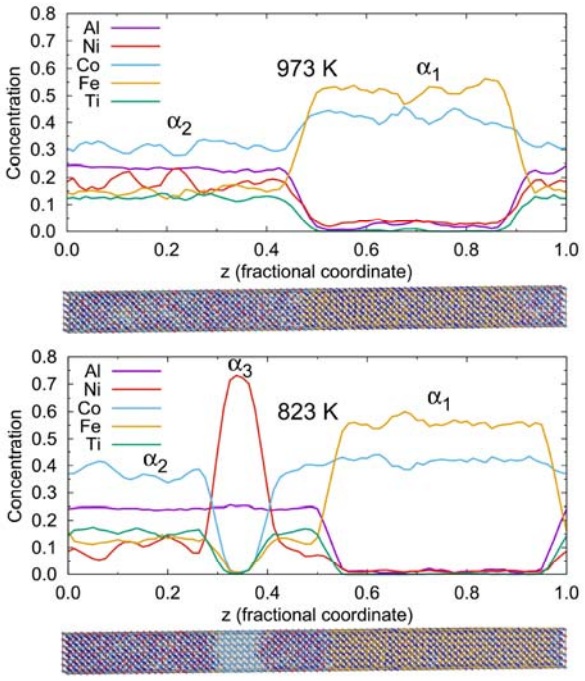

Figure 4. Composition profile of alnico 8 along the z-direction and the corresponding real space atomic structure obtained from MC simulations at (top) 973 and (bottom) 823 K. The silver, light green, blue, gold and red balls in the crystal structure (band beneath each composition profile) indicate the Al, Ni, Co, Fe and Ti atoms.

We also found that if the annealing temperature is further lowered to below 973 K (left part of Fig. 3), there is a 3rd alloy phase appearing in the alnico system. We will refer to this apparently distinct phase as α_3 phase. This α_3 phase consists of mainly Ni and Al with very low concentrations of other transition metal elements (e.g., $Ni_{0.73}Al_{0.25}(FeCoTi)_{0.02}$ at 773K). In Fig. 4, we show composition profiles of each element along the z-direction of the simulation supercell obtained from MC simulations at 973 and 823 K. The compositions of each element at given z-value is calculated as the average on the composition of that element on all sites at that z-value. It is interesting that the concentration of Al is almost constant crossing the α_2 and α_3 phases, indicating that the concentration of Al may be possible to use to manipulate the volume fraction of α_1 magnetic phase in alnico. The α_3 phase has never been reported before. There could be several reasons for that. Firstly, the α_3 phase only appears at quite low annealing temperature in our MC simulations, meaning that it may need a very long annealing at low temperature in an experiment to grow to large enough size to be detectable. Typical time for each step of the low temperature draw process is from several hours to half a day [18], which may not be long enough. Secondly, there could be a high kinetic barrier blocking the formation of α_3 phase although it is thermodynamically stable. Annealing at low temperature does not provide enough kinetics to overcome the barrier. Therefore, the α_3 phase could be quite small in size in comparison to the α_1 and α_2 phases so that it could not be seen clearly in characterization experiment that focuses on the micron-scale structure of alnico 8 and 9 [15,19]. The identification of the α_3 phase in alnico is only possible when all 5 chemical elements are taken into account, showing that quinary CE is indeed needed to study alnico 8 and 9.

We perform kinetically-limited Monte Carlo simulations to understand the effects of short annealing time and slow kinetics at low annealing temperature on the morphology of the structures. Starting with the equilibrium configuration of a high temperature MC simulation (1473 K) as the initial configuration (Fig. S.2 [20]), we only swap 2 randomly picked atoms separated by a distance smaller than 5 or 10 times the lattice constant of a BCC unit cell. These

limited swapping ranges are used to mimic the slow diffusion of atoms in alnico during low temperature annealing. With such simulations, we indeed observed the α_3 phase, which has an Al to transition metals (Fe, Co and Ti together) composition ratio of 1:3 and Ni is richer than all other transition metals. The concentration of Ni increases with the number of MC steps until reaching the saturated concentration. The concentration for Ni in the α_3 phase varies from ~30% to ~75%, depending on the simulation and the α_3 phase is usually quite small long the z-direction of a simulation supercell. If we release the constraint on swapping distance, we can obtain the results discussed above, where there is almost no Fe, Co and Ti in α_3 phase. These results show that the Ni-rich α_3 phase in real alnico samples has a general TM to Al ratio of 3:1 and is small in size, which is consistent with observation of a Ni-enriched rod-shaped phase in commercial alnico 9 [31]. Cu-rich and Ni-rich bridges were also observed in lab alnico samples with composition close to those of commercial alnico 8 and 9 [32] and our results should also be noted for commercial alnico 8 showing Ni-rich clusters/phases (see Supplemental Material [20]). More studies may be needed to clearly clarify the relationship between observed Ni-enriched clusters/phases with the α_3-phase. The success of prediction an alloy phase in a complicated multicomponent alloy at finite temperature in this work is a significant achievement for theoretical materials prediction and design. Most of theoretical predicted and designed materials so far are binary or ternary alloys stabilized at zero temperature.

Now let consider the chemical ordering of 5 constituent elements in α_1, α_2 and α_3 phases of alnico 8 and 9 based on Bragg-William's definition of degree of order [33]. We will consider the ordering of α_1 phase first. From the obtained correlation table (Table S.5 [20]), we observe that the local environment of Fe and Al (Co and Ni) are very similar as both of them have very similar numbers of 1st NN and 2nd NN to other elements, suggesting that if the α_1 phase is in B2 or $D0_3$ order, Fe and Al (Co and Ni) will be in the same sub-lattice. Most of Ti 1st NNs are Ni and Co (7.50 out of 8.00) so that Ti should be on the same sub-lattice with Fe and Al. Therefore, we consider Fe, Al and Ti (Co and Ni) identical in estimating the ordering of α_1 phase. From our occupation scanning, the α_1 phase has B2 order with a degree of order of 77.9% at 773 K and it decreases with temperature, e.g., 52.8% at 973K and 43.8% at 1173K.

From the correlation table of the α_2 phase at 973 K (Table S.6 [20]) we can find that there is no Al-Al and Al-Ti 1st NN or almost no Al-Al 2nd NN, meaning that the α_2 phase is not in the

disordered BCC structure. If the α_2 phase is in B2 order, all Al and Ti should be in a same sub-lattice because there is no Al-Al and Al-Ti 1st NN. Then Al and Ti should be the 2nd NN to themselves and to each other. But there is almost no Al-Al and Ti-Ti 2nd NN, indicating that the α_2 phase is not in the B2 order. The facts that there is no Al-Al and Al-Ti 1st NN, that there is almost no Al-Al and Ti-Ti 2nd NN, that almost all 2nd NN of Al is Fe and Ti (5.64 out of 6.00), and that almost all 3rd NN of Al is Al (10.93 out of 12.00) suggest that the α_2 should be in a $L2_1$ order with all Al on the 4*a*-site and Fe and Ti on 4*b*-site. There could be some anti-site defects and the composition of the α_2 phase is not $L2_1$ stoichiometry (i.e., (NiCo):(FeTi):Al is not 2:1:1 ratio) so that there are some small Al-Ni and Al-Co 2nd NN or the number of Al-Al 3rd NN is not exactly 12.0. Therefore, we can group the 5 elements into 3 groups Ni+Co, Fe+Ti and Al to calculate the correlation table of the "pseudo" ternary. Because there are absolutely no Al-Al 1st NN and a very small number of Al-Al 2nd NN, we can assume (in order to make the estimation of degree of order easier) that all Al of the "pseudo" ternary is on the 4*a*-site of $L2_1$ order if the concentration of Al is less than or equal to 0.25. We then vary the occupations of the other 2 groups on the rest of the 3 sites, i.e., 4*a*-, 4*b*-, and 8*c*-sites, to find the best matching correlation table to the target table calculated for the "pseudo" ternary. The degree of order is then estimated as the degree of order of (Ni+Co) and (Fe+Ti) on the 8*c*- and 4*b*-sites. Our calculation shows that the degree of order of $L2_1$ α_2 phase is very high and it is decreasing with temperature, e.g., 99.2% at 773 K, 92.8% at 973 K and 84.8% at 1173K. The decrease of the degrees of order of α_1 and α_2 phases is coming directly from the increasing of anti-site defects with temperature. Our simulation results related to ordering of α_1 and α_2 phases are in agreement with recent experiments using advanced atomic-scale energy-dispersive X-ray spectra (EDS) mapping techniques [34].

Let's now consider the ordering of the newly identified α_3 phase. The correlation table at 773 K shows clearly that the α_3 phase is not in disordered BCC phase as there is absolutely no Al-Al 1st NN. Thus, the α_3 phase should be in a B2 or $D0_3$ order. The number of 1st NN of Fe and Ti to Al is almost zero so that we can place Co in the same group with Ni and Fe, and that Ti is in the same group with Al, as for the α_1 phase case. The correlation table of "pseudo" binary Ni-Al is shown in Table S.7 [20]. Our occupation scanning shows that the α_3 phase is in a $D0_3$ order with very high degree of order for both temperatures where we observed the α_3 phase, i.e., 99.5% at 773 K and 99.0% at 873 K.

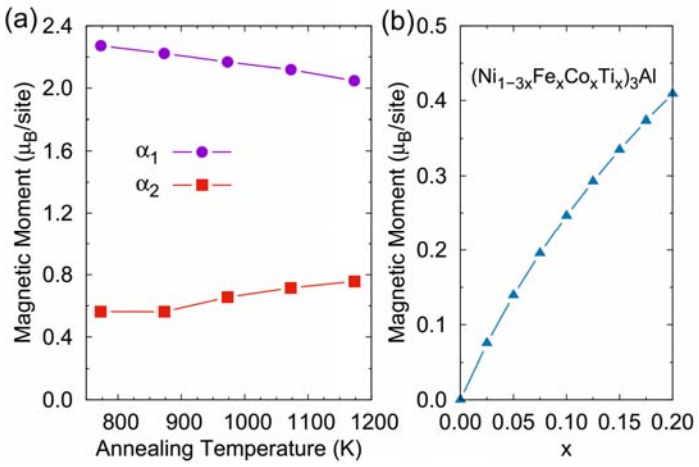

Figure 5. Magnetic moments of (a) α_1 and α_2 phases as function of annealing temperature and (b) that of α_3 phase as a function of TM content in the Ni site.

The magnetic moment per lattice site from DFT calculation within coherent-potential approximation [35–37] as function of annealing temperature for α_1 and α_2 phases is shown in Fig. 5(a). We can see that the magnetic moment of α_1 phase is decreasing with the annealing temperature. In contract, the magnetic moment of α_2 phase is increasing with annealing temperature. This variation of magnetic moment of α_1 (α_2) phase comes directly from the decrease (increase) of magnetic element (Fe and Co) concentrations in α_1 (α_2) phase with the annealing temperature. In both phases, magnetic moments of Fe, Co and Ni are ferromagnetically coupled, while coupling between Ti and other magnetic elements are anti-ferromagnetic. The magnetic moments of Fe and Co are dominant and they are almost constant in each phase, e.g, ~2.75 (~2.50) and ~1.82 (~1.74) μ_B/atom for Fe and Co on α(β)-site in α1 phase and ~ 2.85 μ_B/atom for Fe on 4b-site and ~0.84 for Co on 8c-site in α_2 phase. The magnetic moment of Ti is ~ -0.50 μ_B/atom in α_2 phase. The magnetic moment of Ni is ~ 0.62 μ_B/atom in α_1 phase and ~ 0.20 μ_B/atom in α_2 phase. These results are similar to those of alnico 5-7 [9]. However, the concentration of Co in alnico 5-7 is much smaller than that in alnico 8, making a much smaller magnetic moment for α_2 phase in alnico 5-7, about half of that in alnico 8, which is being considered here. Figure 5(b) shows the magnetic moment of α_3 phase with Ni substituted for other TMs: $D0_3$ $(Ni_{1-3x}Fe_xCo_xTi_x)_3Al$ with $0 \leq x \leq 0.2$. For simplicity, we assume the same concentrations for Fe, Co and Ti. The magnetic moment of the α_3 phase increases monotonically with the concentration of other TMs on the Ni sites. For $x > 0$, Fe, Co and Ni also exhibit ferromagnetic coupling among themselves and anti-ferromagnetically coupled with Ti.

The magnetic moment of Fe and Co are dominant, i.e., at x = 0.20 magnetic moments of Fe, Co, Ni and Ti are 1.92, 0.87, 0.12 and -0.21 μ_B/atom, respectively. At very high substitution concentration (x = 0.20), the magnetic moment of α_3 phases is still small (0.41 μ_B/site), which is much smaller than that of α_1 phase and is about two thirds of that of α_2 phase at 773 K.

Above MC simulations and magnetic calculations show that magnetism in the α_2 phase is inevitable due to high Co concentration in α_2 phase. The magnetism of the α_2 phase lessens the magnetic isolation between needles of α_1 phase and lowers the coercivity of alnico as mentioned above. The newly identified α_3 phase, appearing at low annealing temperature, provides clue for a possible way to overcome magnetism issue in the α_2 phase. If we can achieve the enrichment of Ni in α_3 phase precipitating at the boundary of α_1 and α_2 phases during low temperature annealing, a very weak magnetic "*skin layer*" would be developed to wrap the α_1 needles. Hence, the α_1 magnetic needles will be magnetically well decoupled from each other, then the coercivity of alnico will be enhanced. Recent experimental work on alnico showed the signal of this "*skin layer*" [32]. Our results suggest that substitution of Co by Ni or co-substitution of Co by Ni-Fe or Ni-Al pairs, a similar concept of co-doing in semiconductor, to lower Co concentration and to provide more Ni for α_3 phase to develop, together with a redesign of draw process to include lower temperature annealing would enhance the formation of the α_3 phase. This substitution could reduce un-wanted Co in α_2 phase and it also lower the cost of alnico as Co is more costly than other metals like Fe, Al and Ni in alnico.

In summary, we developed an accurate and transferable quinary alloy cluster expansion model. Monte Carlo simulations were performed to study the atomic structures of alnico 8 and 9 at atomistic and nano scales as a function of annealing temperature. The simulation results on phase separation and phase selection are in agreement with experiment. More details on the ordering in each separated phase of alnico were provided: the α_1 phase is in B2 order with Ni and Co preferring the same sub-lattice site; the α_2 phase is in $L2_1$ order with Ni and Co preferring the 8*c*-site and Al occupying 4*a*-site. A previously un-recognized 3rd alloy phase was predicted by Monte Carlo simulations and was confirmed by experiment. The new alloy phase is rich in Ni, has TM:Al ratio of 3:1, is, in general, in $D0_3$ TM_3Al order, and exhibits very weak magnetization. The identification of the α_3 phase gives a possible route to enhance magnetic

properties of alnico by controlling the processing conditions to manipulate the size and locations of the α_3 phase.

ACKNOWLEDGEMNETS

The U.S. Department of Energy, Office of Energy Efficiency and Renewable Energy, Vehicle Technologies Office, Electric Drive Technologies Program supported the research at the Ames Laboratory, which is operated for the DOE by Iowa State University under Contract No. DE-AC02-07CH11358. We also acknowledge computing time support at the National Energy Research Scientific Computing Center (NERSC).

*Email: mcnguyen@ameslab.gov

REFERENCES

[1] N. Metropolis and S. Ulam, *The Monte Carlo Method*, J. Am. Stat. **44**, 335 (1949).

[2] W. Kohn and L. J. Sham, *Self-Consistent Equations Including Exchange and Correlation Effects*, Phys. Rev. **140**, A1133 (1965).

[3] J. M. Sanchez, F. Ducastelle, and D. Gratias, *Generalized cluster description of multicomponent systems*, Phys. A Stat. Mech. Its Appl. **128**, 334 (1984).

[4] A. van de Walle, *Multicomponent multisublattice alloys, nonconfigurational entropy and other additions to the Alloy Theoretic Automated Toolkit*, Calphad Comput. Coupling Phase Diagrams Thermochem. **33**, 266 (2009).

[5] C. Wolverton and D. De Fontaine, *Cluster expansions of alloy energetics in ternary intermetallics*, Phys. Rev. B **49**, 8627 (1994).

[6] A. Van der Ven and G. Ceder, *Vacancies in ordered and disordered binary alloys treated with the cluster expansion*, Phys. Rev. B **71**, 54102 (2005).

[7] J. S. Wróbel, D. Nguyen-Manh, M. Y. Lavrentiev, M. Muzyk, and S. L. Dudarev, *Phase stability of ternary fcc and bcc Fe-Cr-Ni alloys*, Phys. Rev. B **91**, 24108 (2015).

[8] F. Lechermann, M. Fahnle, and J. M. Sanchez, *First-principles investigation of the Ni-Fe-Al system*, Intermetallics **13**, 1096 (2005).

[9] W. P. Huhn and M. Widom, *Prediction of A2 to B2 Phase Transition in the High-Entropy Alloy Mo-Nb-Ta-W*, JOM **65**, 1772 (2013).

[10] M. C. Nguyen, X. Zhao, C.-Z. Wang, and K.-M. Ho, *Cluster expansion modeling and Monte Carlo simulation of alnico 5–7 permanent magnets*, J. Appl. Phys. **117**, 93905 (2015).

[11] S. B. Maisel, M. Höfler, and S. Müller, *Configurationally exhaustive first-principles study of a quaternary superalloy with a vast configuration space*, Phys. Rev. B **94**, 14116

(2016).

[12] I. Toda-Caraballo, J. S. Wróbel, S. L. Dudarev, D. Nguyen-Manh, and P. E. J. Rivera-Díaz-del-Castillo, *Interatomic spacing distribution in multicomponent alloys*, Acta Mater. **97**, 156 (2015).

[13] R. W. McCallum, L. Lewis, R. Skomski, M. J. Kramer, and I. E. Anderson, *Practical Aspects of Modern and Future Permanent Magnets*, Annu. Rev. Mater. Res. **44**, 451 (2014).

[14] M. J. Kramer, R. W. McCallum, I. A. Anderson, and S. Constantinides, *Prospects for non-rare earth permanent magnets for traction motors and generators*, Jom **64**, 752 (2012).

[15] L. Zhou, M. K. Miller, P. Lu, L. Ke, R. Skomski, H. Dillon, Q. Xing, A. Palasyuk, M. R. McCartney, D. J. Smith, S. Constantinides, R. W. McCallum, I. E. Anderson, V. Antropov, and M. J. Kramer, *Architecture and magnetism of alnico*, Acta Mater. **74**, 224 (2014).

[16] J. W. Cahn, *On spinodal decomposition*, Acta Metall. **9**, 795 (1961).

[17] J. W. Cahn, *Magnetic aging of spinodal alloys*, J. Appl. Phys. **34**, 3581 (1963).

[18] M. Stanek, L. Wierzbicki, and M. Leonowicz, *Investigations of Thermo-Magnetic Treatment of Alnico 8 Alloy*, Arch. Metall. Mater. **55**, 571 (2010).

[19] Q. Xing, M. K. Miller, L. Zhou, H. M. Dillon, R. W. McCallum, I. E. Anderson, S. Constantinides, and M. J. Kramer, *Phase and elemental distributions in alnico magnetic materials*, IEEE Trans. Magn. **49**, 3314 (2013).

[20] Supplementary Material, *Supplementary Material* (2017).

[21] A. van de Walle and G. Ceder, *Automating first-principles phase diagram calculations*, J. Phase Equilibria **23**, 348 (2002).

[22] G. Kresse and J. Furthmüller, *Efficient iterative schemes for ab initio total-energy calculations using a plane-wave basis set*, Phys. Rev. B **54**, 11169 (1996).

[23] P. E. Blöchl, *Projector augmented-wave method*, Phys. Rev. B **50**, 17953 (1994).

[24] G. Kresse and D. Joubert, *From Ultrasoft Pseudopotentials to the Projector Augmented Wave Method*, Phys. Rev. B **59**, 1758 (1999).

[25] J. P. Perdew, K. Burke, and M. Ernzerhof, *Generalized Gradient Approximation Made Simple*, Phys. Rev. Lett. **77**, 3865 (1996).

[26] H. J. Monkhorst and J. D. Pack, *Special points for Brillouin-zone integrations*, Phys. Rev. B **13**, 5188 (1976).

[27] P. B. Budberg and A. Prince, in edited by G. Petzow and G. Effenberg (VCH, Weinheim, 1991), pp. 309–323.

[28] V. Y. Markiv, *Phase equilibrium in the Ti-Co-Al system*, Russ. Met. **1**, 84 (1966).

[29] J. J. Ding, P. Rogl, and H. Schmidt, *Phase relations in the Al-rich corner of the Ti–Ni–Al system*, J. Alloys Compd. **317–318**, 379 (2001).

[30] K. Zeng, R. Schmid-Fetzer, B. Huneau, P. Rogl, and J. Bauer, *The ternary system Al–Ni–*

Ti Part II: thermodynamic assessment and experimental investigation of polythermal phase equilibria, Intermetallics **7**, 1347 (1999).

[31] L. Zhou, M. Miller, D. A. Cullen, P. Lu, R. W. McCallum, I. E. Anderson, S. Constantinides, and M. J. Kramer, *Microstractural characterization of alnico 9 alloy*, Microsc. Microanal. **21**, 1343 (2015).

[32] M. Fan, Y. Liu, R. Jha, G. S. Dulikravich, J. Schwartz, and C. Koch, *On the Formation and Evolution of Cu-Ni-rich Bridges of Alnico Alloys with Thermomagnetic Treatment*, IEEE Trans. Magn. **52**, 1 (2016).

[33] W. L. Bragg and E. J. Williams, *The Effect of Thermal Agitation on Atomic Arrangement in Alloys*, Proc. R. Soc. A Math. Phys. Eng. Sci. **145**, 699 (1934).

[34] P. Lu, L. Zhou, M. J. Kramer, and D. J. Smith, *Atomic-scale chemical imaging and quantification of metallic alloy structures by energy-dispersive X-ray spectroscopy.*, Sci. Rep. **4**, 3945 (2014).

[35] R. J. Elliott, J. A. Krumhansl, and P. L. Leath, *The theory and properties of randomly disordered crystals and related physical systems*, Rev. Mod. Phys. **46**, 465 (1974).

[36] H. Ebert et al, *The Munich SPR-KKR package, Version 6.3*, (2012).

[37] H. Ebert, D. Ködderitzsch, and J. Minár, *Calculating condensed matter properties using the KKR-Green's function method—recent developments and applications*, Reports Prog. Phys. **74**, 96501 (2011).